

Post-Synthetic Modification of a Porous Hydrocarbon Cage to Give a Discrete Co_{24} Organometallic Complex**

Chriso M. Thomas,^[a] Weibin Liang,^[b] Dan Preston,^[a] Christian J. Doonan,^[b] and Nicholas G. White*^[a]

Abstract: A new alkyne-based hydrocarbon cage was synthesized in high overall yield using alkyne-alkyne coupling in the cage forming step. The cage is porous and displays a moderately high BET surface area ($546 \text{ m}^2 \text{ g}^{-1}$). The cage loses crystallinity on activation and thus is porous in its amorphous

form, while very similar cages have been either non-porous, or retained crystallinity on activation. Reaction of the cage with $\text{Co}_2(\text{CO})_8$ results in exhaustive metalation of its 12 alkyne groups to give the $\text{Co}_{24}(\text{CO})_{72}$ adduct of the cage in good yield.

Introduction

The design, synthesis and application of cage molecules is of considerable interest due to the unusual and beneficial properties conveyed by the rigid internal pore of these cages. Many cages are assembled through metal-ligand coordination bonds,^[1] while another large group of materials are assembled using reversible covalent bond forming reactions such as imine or boronate ester condensations.^[2] A smaller group of cages have been prepared using irreversible covalent bond forming reactions such as oxidative coupling of alkynes,^[3] while these have relatively lower yields due to the lack of an error correction mechanism, the resulting cages tend to be highly robust.^[4] Additionally, this irreversible chemistry offers potential advantages when it comes to subsequent modification of the cages and/or synthesizing cages with low symmetry.

Due to their large internal pores, cages are potentially permanently porous materials, although in practice realizing porous materials is difficult and often unpredictable. This is because it relies on the cages packing such that voids are aligned and crystal engineering the weak packing interactions between cages is challenging. Several groups have attempted

to gain more predictability by deliberately attempting to guide the packing of cages,^[5] although this is extremely challenging. To illustrate these challenges: a few years ago one of us reported the covalent cage 2^{OMe} (Figure 1), this cage is non-porous to nitrogen when slowly crystallized as the pores in the crystal structure do not align. In contrast, the cage is highly porous when rapidly precipitated from solution (which results in a crystalline material).^[3b] Interestingly, replacing the methoxy groups with bromines (i.e. 2^{Br}) resulted in a non-porous

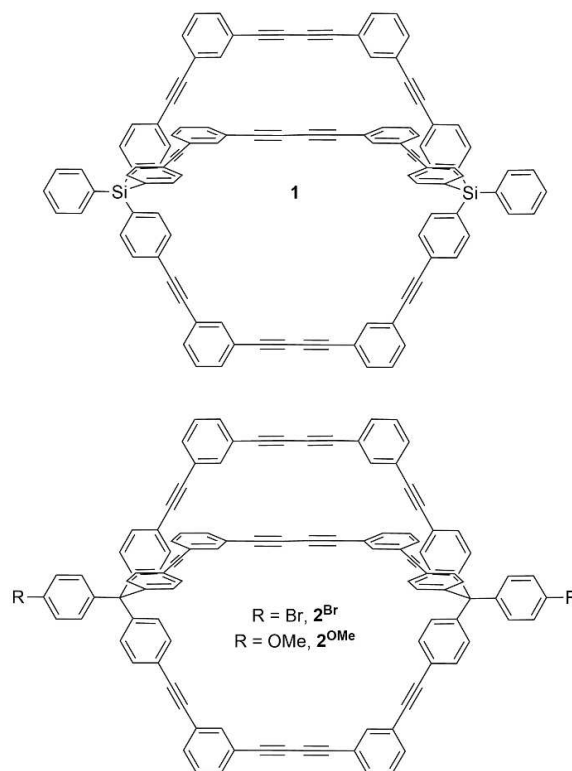


Figure 1. Structure of new cage **1** and previously-reported cages 2^{OMe} and 2^{Br} .

[a] Dr. C. M. Thomas, Dr. D. Preston, Assoc. Prof. N. G. White
Research School of Chemistry
The Australian National University
Canberra, ACT (Australia)
E-mail: nicholas.white@anu.edu.au
Homepage: www.nwhitegroup.com

[b] Dr. W. Liang, Prof. C. J. Doonan
Department of Chemistry and Centre for Advanced Materials
The University of Adelaide, SA (Australia)

[**] A previous version of this manuscript has been deposited on a preprint server (<https://doi.org/10.26434/chemrxiv-2022-9gw50>).

Supporting information for this article is available on the WWW under <https://doi.org/10.1002/chem.202200958>

© 2022 The Authors. Chemistry - A European Journal published by Wiley-VCH GmbH. This is an open access article under the terms of the Creative Commons Attribution Non-Commercial NoDerivs License, which permits use and distribution in any medium, provided the original work is properly cited, the use is non-commercial and no modifications or adaptations are made.

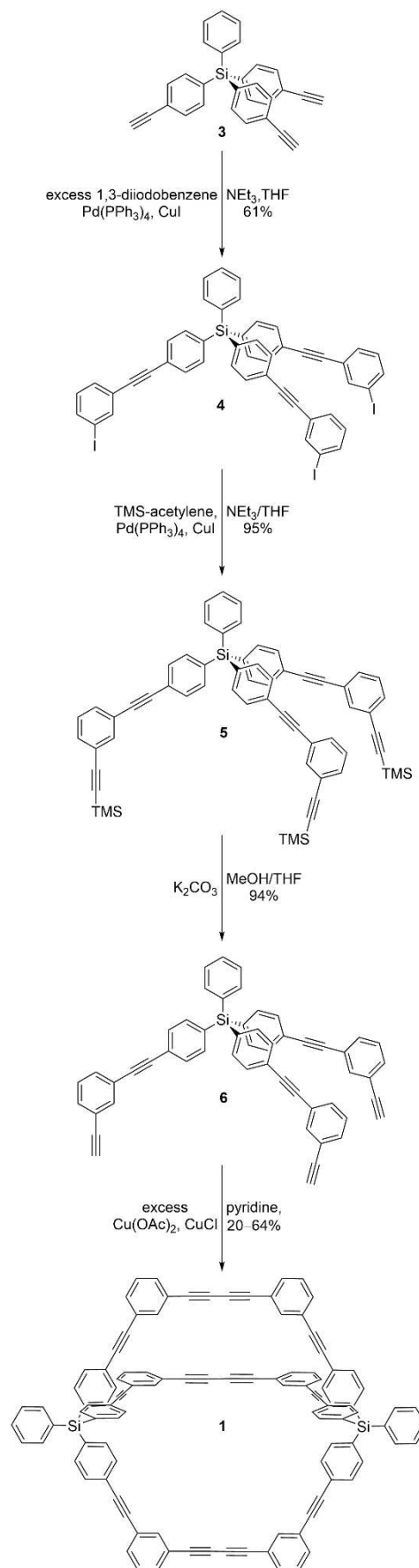
material.^[6] Clearly, very small changes in cage structure can lead to very different materials properties.

As is the case with extended framework structures,^[7] it is often convenient to synthesize organic cages and then post-synthetically modify these to incorporate additional functionality.^[8] Most of the reported examples of post-synthetic modification have described organic reactions to give new cage properties,^[9] or to network discrete cages into polymeric structures. There have been a small number of reports of post-synthetic metalation of cages, and many of these have been used to form either nanoparticles inside the cage,^[10] or to link organic cages into metal-organic frameworks.^[11] There are a few reports of metalations of organic cages to give well-defined transition metal complexes: these have involved coordination of up to six metal centres to amine, imine or porphyrin donors of organic cages,^[12] but we are not aware of higher nuclearity metal complexes prepared in this manner.

Many porous organic cages contain numerous alkyne groups,^[3,4a,b] which seem to be ripe for post-synthetic modification. We hypothesized that they could be used to coordinate to transition metals to provide well-defined polynuclear cluster complexes, i.e. the cage could be used as a ligand to construct large, well-defined architectures. These clusters may have interesting materials properties due to their large bulk and inability to pack efficiently, which would be expected to lead to extrinsic porosity in addition to the intrinsic porosity provided by the cage cavity. In this work, we report the efficient synthesis of the new cage 1, which contains twelve alkyne groups. We investigate its porosity, and demonstrate that it can be converted in one step and high yield into a Co₂₄ complex through coordination of cobalt carbonyl to the alkyne groups.^[13] We believe that this represents the highest nuclearity discrete complex prepared by metalation of an organic cage.

Results and Discussion

Synthesis of 1: In order to allow a full study of the properties of cage 1 and related cages, we first optimized its synthesis. Scheme 1 shows the synthesis of the tris-alkyne “half-cage” precursor: we opted to build our cages on tetraphenylsilane scaffolds due to the ease of synthesizing these with appropriate substituents. We initially investigated several synthetic routes but in the end found that the best approach was to form the tetraphenylsilane group and subsequently derivatize this (see Supporting Information for details of alternative synthetic pathways investigated). We found that the known tris-alkyne 3 could be prepared efficiently in high yields (73% overall yield from commercially available materials, see Supporting Information). Reacting 3 with ten equivalents of diiodobenzene gave tris-iodide 4 in 61% yields without the need for monoprotection. A final coupling/deprotection reaction with TMS-acetylene gave the target tris-alkyne 6. Notably this synthesis gives ready access to the half-cage 6 on large scales and in 40% overall yield from inexpensive commercial reagents (1,4-dibromobenzene and tris-ethoxyphenylsilane), and compares favourably in



Scheme 1. Synthesis of cage 1.

terms of yield and length of synthesis with other alkyne-based cages.^[3a–c,e]

Having access to **6**, we next attempted to synthesize the target cage **1** through oxidative alkyne coupling reactions (Scheme 1). It was found that adding a solution **6** in pyridine dropwise to heated solution containing a large excess of anhydrous $\text{Cu}(\text{OAc})_2$ and CuCl in pyridine gave the cage in relatively high yields after purification by preparative TLC. The best yield we obtained was 64%, which is surprisingly high given that three bonds are formed through irreversible reactions and there is considerable scope for “wrong” steps during this process. We note that this means the overall yield for the multi-step synthesis of the cage is 25% from cheap commercially-available starting materials. However, the cage formation reaction suffers from poor reproducibility and poor scalability, for example yields of ~20% obtained when 0.30 mmol scales (i.e. ~200 mg of **6**) were used. Nevertheless, significant quantities of pure cage could be obtained, which were characterized by ^1H and ^{13}C NMR spectroscopy, high resolution mass spectrometry and X-ray crystallography.

Solid state structure of 1: Small single crystals of **1** could be obtained by slow evaporation of a dichloromethane/petroleum spirits solution, and these were characterized by synchrotron X-ray crystallography. The molecule crystallizes in the monoclinic space group $C2/c$ with two independent cage molecules in the asymmetric unit. A well resolved *n*-hexane molecule is located between the two cage molecules; the asymmetric unit also contains large voids containing diffuse electron density, which were included in the model using PLATON-SQUEEZE.^[14] Using this programme, we were able to estimate that 44% of the unit cell is made up of solvent-filled voids (in addition to the space occupied by the well-ordered hexane molecule), and these voids form channels through the structure (Figure 2). The silicon atoms have angles very close to ideal tetrahedra (i.e. 109.5°), as is common for tetraphenylsilane groups.^[15] In contrast, the phenyl/alkyne parts of the cages distort significantly resulting in a structure that deviates substantially from idealized D_{3h} symmetry (Figure 2).

Gas sorption properties of 1: While the crystal structure of **1** reveals that the cage has aligned pores, we found that the compound loses crystallinity and becomes amorphous upon drying (as indicated by PXRD). To examine whether this material is porous, we studied its nitrogen sorption at 77 K. These studies revealed a Type I isotherm with minor hysteresis in the desorption process at low pressure, which is typical for these kinds of amorphous porous organic materials (Figure 3).^[16] The BET surface area of **1** is $546 \text{ m}^2 \text{ g}^{-1}$, which is relatively high for a purely organic material, although less than was observed for the porous polymorph of the related compound 2^{OMe} ($1153 \text{ m}^2 \text{ g}^{-1}$).^[3b]

Taken together, the cages **1**, 2^{OMe} and 2^{Br} exemplify the significant challenges that remain in predicting the porosity of organic cages. The molecular structures of these three cages feature only very minor differences as can be seen by the overlay of the crystal structures of **1** and 2^{OMe} (Figure 2c), and yet they display markedly different porosity properties. 2^{OMe} has a kinetically-favoured porous polymorph that retains its crystal-

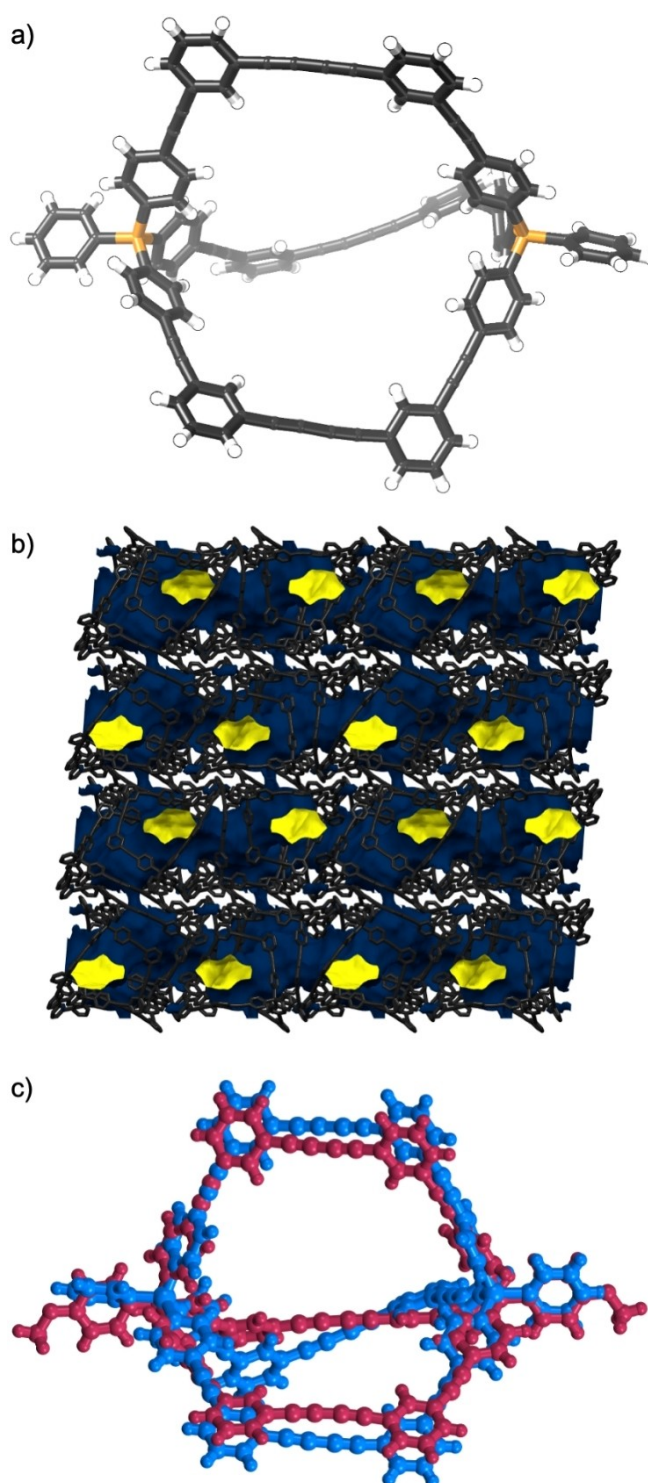


Figure 2. X-ray crystal structure of **1**: a) lower-numbered cage molecule ($Z' = 2$), in each case the two silicon atoms sit horizontally to emphasize the distortions from ideal D_{3h} symmetry; b) solvent accessible voids in the packing diagram of **1** (calculated using a probe radius of 1.82 Å); c) overlay of lower-numbered cage molecule in the structure of **1** (blue) with the X-ray crystal structure of 2^{OMe} (maroon, CCDC: 913184).^[3b]

linity on drying,^[3b,17] as well as a thermodynamically-favoured crystalline polymorph that is non-porous, while 2^{Br} is non-

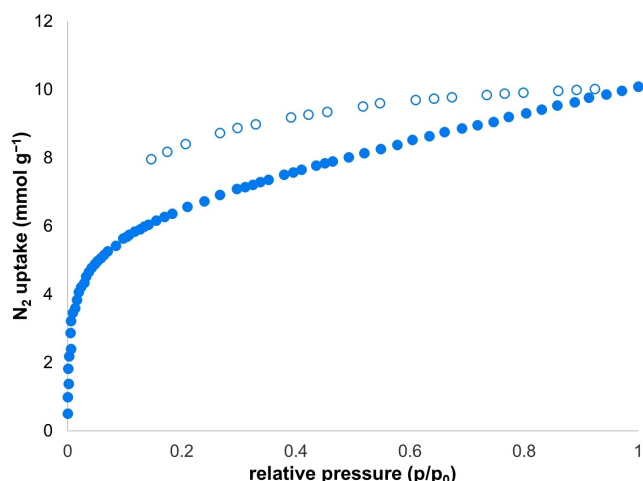


Figure 3. Nitrogen sorption isotherms of **1** at 77 K (filled circles represent adsorption, open circles represent desorption).

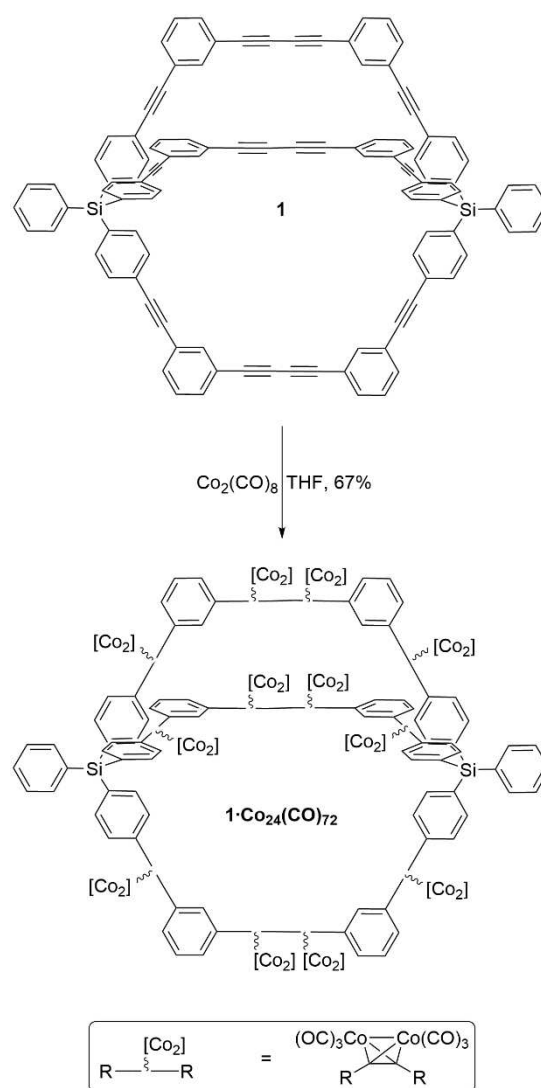
porous.^[6] The new cage **1** is porous, but unlike **2^{OMe}** is porous in an amorphous form.

Synthesis of 1·Co₂₄(CO)₇₂: Having shown that **1** is porous, we next sought to investigate whether it could be post-synthetically modified by reaction with dicobalt octacarbonyl. In general, this reaction proceeds in very high yields and mild reaction conditions, and discrete compounds with up to 16 cobalt centres have been reported through the reaction of Co₂(CO)₈ with a resorcinarene-based octa-alkyne.^[18] Cage molecule **1** contains twelve alkyne units, so theoretically could react with 12 molecules of Co₂(CO)₈ to form **1·Co₂₄(CO)₇₂**. Reacting **1** with an excess (20 equivalents) of Co₂(CO)₈ in dry THF in the dark at room temperature followed by work-up gave a single species in good yield (67%, Scheme 2). This product was characterized by ¹H and ¹³C NMR spectroscopy, IR spectroscopy and high resolution ESI mass spectrometry.

¹H NMR spectroscopy showed the disappearance of the starting cage and broadening of some resonances, while ¹³C NMR spectroscopy showed the disappearance of the four resonances corresponding to the alkyne groups of **1**. Four new downfield-shifted resonances appear at 91.5–99.3 ppm, which we attribute to coordinated alkynes (Figure 4). Two peaks are observed with an approximate 1:1 ratio at 199.0 and 199.5 ppm, consistent with six Co₂(CO)₆ units in each of two possible environments (coordinated to either diphenylacetylene or butadiyne groups). Only one ¹³C resonance is observed for each of these environments, as expected.^[19]

Strong carbonyl stretching frequencies are observed in the IR spectrum at 2091, 2052 and 2022 cm⁻¹, while the absence of a peak corresponding to a bridging carbonyl at ~1860 cm⁻¹^[20] indicates complete removal of excess Co₂(CO)₈. Further evidence for exhaustive metalation to give **1·Co₂₄(CO)₇₂** was provided by high resolution ESI mass spectrometry, which showed peaks corresponding to the sodium adduct of **1·Co₂₄(CO)₇₂**.

Taken together, ¹H and ¹³C NMR, and IR spectroscopy as well as high resolution mass spectrometry all provide strong



Scheme 2. Synthesis of **1·Co₂₄(CO)₇₂**.

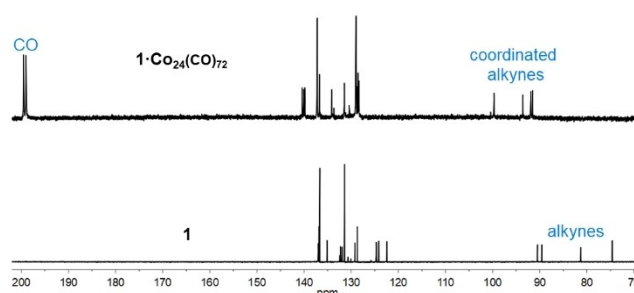


Figure 4. Partial ¹³C NMR spectra of **1** and **1·Co₂₄(CO)₇₂** (CD₂Cl₂, 298 K, 151 MHz).

evidence for the formation of the targeted Co₂₄ complex. Unfortunately, the stability of the material is limited with the initially-formed red-brown powder turning black over time. Due to these stability limitations, we were unable to evaluate the gas uptake of **1·Co₂₄(CO)₇₂**, and despite numerous attempts

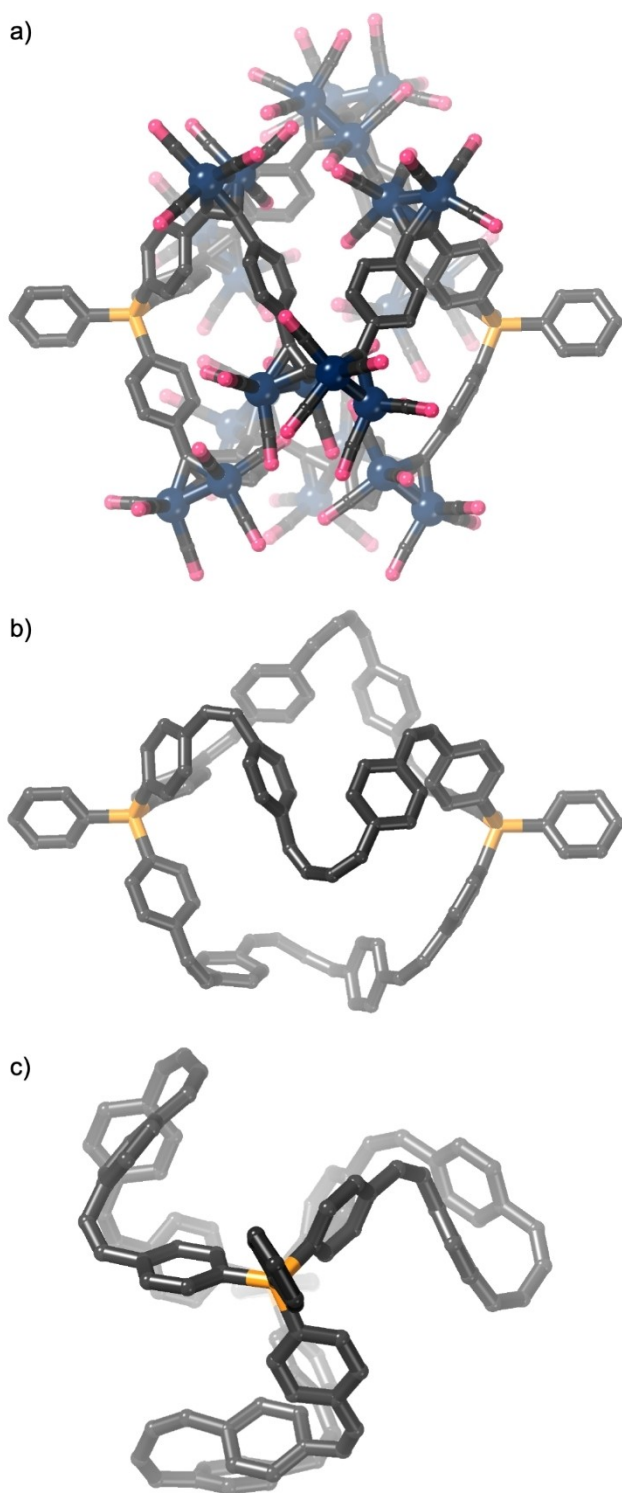


Figure 5. Energy minimized structure of $1\text{-Co}_{24}(\text{CO})_{72}$ (semi-empirical, GFN2-xTB^[22]): a) full structure, b) and c) views of the carbon skeleton of the structure.

were unable to obtain single crystals suitable for X-ray crystallography experiments.

Given the known instability of dicobalt adducts of alkynes, we attempted to stabilize these motifs by addition of chelating

bis(diphenylphosphino)methane (**dppm**) ligands.^[21] Unfortunately, either the direct reaction of **1** with $\text{Co}_2(\text{CO})_6\text{dppm}$ or reaction of $1\text{-Co}_{24}(\text{CO})_{72}$ with **dppm** did not lead to the desired product $1\text{-Co}_{24}(\text{CO})_{48}(\text{dppm})_{12}$. Presumably the steric demands of the rigid and bulky $\text{Co}_2(\text{CO})_4\text{dppm}$ units are too great to allow the reaction to go to completion. While unsuccessful in this case, it is suggested that this approach may be viable for other cages containing fewer, or more separated, alkyne motifs.

Computational modelling of $1\text{-Co}_{24}(\text{CO})_{72}$: We used the GFN2-xTB semi-empirical method^[22] implemented within xTB^[23] to gain insight into the structure and dynamics of $1\text{-Co}_{24}(\text{CO})_{72}$ in implicit dichloromethane solvent. After an initial energy minimization, we conducted short molecular dynamics simulations at a semi-empirical level of theory to generate potential low energy geometries. The lowest energy structure identified in the molecular dynamics simulations was then further optimised (see Supporting Information for full details). Importantly the minimized structure (Figure 5) reproduces well the key geometric features of crystallographically characterized alkyne- $\text{Co}_2(\text{CO})_6$ complexes (Table S2). Additionally the calculated IR spectrum for the modelled complex is very similar to the experimentally observed spectrum of $1\text{-Co}_{24}(\text{CO})_{72}$ (Figure S27).

All low energy structures identified had *cis* conformation of all coordinated alkyne units, presumably to minimise steric strain. Surveys of the Cambridge Structural Database^[24] indicated that this is common, with all $\text{Co}_2(\text{CO})_6$ complexes of diphenylacetylene adopting a *cis* conformation and approximately half of $\text{Co}_2(\text{CO})_6$ complexed butadiyne structures taking on the *cis-cis-cis* conformation observed in the modelled structure of $1\text{-Co}_{24}(\text{CO})_{72}$. Looking at the modelled structure, it is perhaps unsurprising that attempts to coordinate **dppm** to the $\text{Co}_2(\text{CO})_6$ units were unsuccessful due to the steric demands that this would place on an already congested structure.

Conclusion

We have described the synthesis of the new cage **1**. Incorporating a silicon atom into the “half-cage” building block **6** allowed for an efficient synthesis, although the yields of the cage-forming reaction were variable. The cage loses crystallinity upon activation but the amorphous cage displays moderately high porosity (BET surface area: $546\text{ m}^2\text{ g}^{-1}$). Cage **1** contrasts with the related cages **2^{OMe}** and **2^{Br}**, one of which is porous but only when rapidly precipitated, and the other of which is non-porous.

Reaction of **1** with $\text{Co}_2(\text{CO})_8$ resulted in the exhaustive metalation of the twelve alkyne groups to cleanly give the organometallic Co_{24} complex, thus demonstrating an effective route to well-defined high nuclearity metal clusters. This approach is complementary to the use of organometallic bond formation to form metal-organic cages, i.e. those where the cage is formed through M–C bonds.^[25] Unfortunately $1\text{-Co}_{24}(\text{CO})_{72}$ has limited stability, but the high yielding and clean post-synthetic modification of the cage suggests that a similar synthetic approach may be more successful for other

related cages, particularly if subsequent chelating ligands such as **dppm** could also be incorporated to enhance stability. Such post-synthetically metallated cages may well be highly porous as their large and bulky nature means that they are unlikely to be able to pack efficiently.

Experimental Section

General remarks: Full details of synthesis and characterization are provided as Supporting Information. This includes details of instrumentation, NMR spectra of new compounds, details of alternative synthetic pathways investigated, an optimized route to **3** and details of X-ray crystallography.

Deposition Number(s) 2157097 contain(s) the supplementary crystallographic data for this paper. These data are provided free of charge by the joint Cambridge Crystallographic Data Centre and Fachinformationszentrum Karlsruhe Access Structures service.

Synthesis of tris-iodo compound 4: A mixture of 1,3-diiodobenzene (3.1 g, 9.3 mmol), Pd(PPh₃)₄ (0.23 g, 0.20 mmol), CuI (0.038 g, 0.20 mmol) in NEt₃ (18 mL) was cooled to 0 °C. Tris-alkyne **3** (0.38 g, 0.93 mmol) was dissolved in THF (8 mL) and was added dropwise to the reaction mixture, which was then stirred overnight at room temperature under a nitrogen atmosphere. The solvent was removed under reduced pressure, and the resulting solid was dissolved in dichloromethane (120 mL) and washed with water (50 mL) and brine (50 mL). The organic extract was dried over MgSO₄ and taken to dryness under reduced pressure. Purification by column chromatography (1:5 DCM:pet. spirits) gave **4** as white flakes. Yield: 0.58 g (0.57 mmol, 61%). ¹H NMR (CDCl₃, 400 MHz): 7.90 (t, *J* = 1.7 Hz, 3H), 7.66–7.69 (m, 3H), 7.39–7.56 (m, 20H), 7.09 (t, *J* = 7.9 Hz, 3H) ppm. ¹³C NMR (CDCl₃, 101 MHz): 140.3, 137.6, 136.5, 136.4, 134.5, 132.9, 131.2, 130.9, 130.0, 128.3, 128.2, 125.3, 124.5, 93.8, 90.7, 89.1 pm. HRESI-MS (pos.): 1013.9186, calc. for [C₄₈H₂₉SiI₃]⁺, i.e. [M]⁺ = 1013.9173 Da.

Synthesis of tris-TMS alkyne 5: Compound **4** (0.60 g, 0.59 mmol), Pd(PPh₃)₄ (0.017 g, 0.010 mmol), and CuI (0.0019 g, 0.010 mmol) were stirred in NEt₃ (12 mL). Trimethylsilylacetylene (0.40 mL, 2.3 mmol) was added, and the mixture was stirred overnight at room temperature under a nitrogen atmosphere. The solvent was removed under reduced pressure, and the resulting solid was dissolved in dichloromethane (70 mL) and washed with water (30 mL) and brine (30 mL). The organic extract was dried over MgSO₄ and taken to dryness under reduced pressure. Purification by column chromatography (1:8 DCM:pet. spirits) gave **5** as white flakes. Yield: 0.52 g (0.56 mmol, 95%). ¹H NMR (CDCl₃, 400 MHz): 7.66 (s, 3H), 7.39–7.56 (m, 23H), 7.29 (t, *J* = 7.8 Hz, 3 H), 0.25 (s, 27H) ppm. ¹³C NMR (CDCl₃, 101 MHz): 136.5, 136.4, 135.2, 134.3, 133.1, 131.9, 131.7, 131.1, 130.2, 128.5, 128.3, 124.7, 123.7, 123.5, 104.2, 95.2, 89.9, 0.1 ppm (one alkyne peak not observed due to peak overlap). HRESI-MS (pos.): 924.3458, calculated for [C₆₃H₅₆Si₄]⁺, i.e. [M]⁺ = 924.3459 Da.

Synthesis of tris-alkyne 6: K₂CO₃ (0.35 g, 2.6 mmol) was added to a solution of **5** (0.60 g, 0.65 mmol) in 1:1 THF:MeOH (20 mL) and the mixture was stirred for 5 h at room temperature under a nitrogen atmosphere. The solvent was removed under reduced pressure and the resulting solid was dissolved in dichloromethane (70 mL), and washed with water (2 × 30 mL) and brine (30 mL). The organic phase was dried over MgSO₄ and the solvent removed under reduced pressure to give **6** as fine yellow powder. Yield: 0.43 g (0.61 mmol, 94%). ¹H NMR (CDCl₃, 400 MHz): 7.68 (t, *J* = 1.4 Hz, 3H), 7.40–7.57 (m, 23H), 7.32 (t, *J* = 7.8 Hz, 3H), 3.10 (s, 3H) ppm. ¹³C NMR (CDCl₃, 101 MHz): 136.5, 136.4, 135.3, 134.4, 133.0, 132.10, 132.06,

131.2, 130.2, 128.6, 128.3, 124.6, 123.6, 122.7, 90.1, 89.8, 82.9, 78.0 ppm. HRESI-MS (pos.): 708.2271, calculated for [C₅₄H₃₂Si]⁺, i.e. [M]⁺ = 708.2273 Da.

Synthesis of cage 1: A Schlenk flask was charged with Cu(OAc)₂·H₂O (0.46 g, 2.3 mmol) and this was dried at 70 °C for two hours under vacuum. CuCl (0.16 g, 1.6 mmol) and dry pyridine (30 mL) were added. Then a solution of **6** (0.025 g, 0.035 mmol) dissolved in dry pyridine (30 mL) was added dropwise to this mixture at 80 °C and stirred at this temperature for 2 h. The reaction mixture was stirred overnight at room temperature under a nitrogen atmosphere and the solvent was then removed under vacuum. The residue was extracted with dichloromethane (200 mL) and washed with 1.0 M HCl(aq) (50 mL) and water (2 × 50 mL). The organic extract was dried over MgSO₄ and concentrated under reduced pressure. It was then purified by preparative TLC (1:2 DCM:pet. spirits) to give **1** as a pale yellow powder. Yield: 0.016 g (0.011 mmol, 64%). ¹H NMR (CDCl₃, 400 MHz): 7.77 (br. s, 6H), 7.69 (dd, *J* = 7.8, 1.3 Hz, 4H), 7.44–7.56 (m, 42H), 7.33 (t, *J* = 7.8 Hz, 6H) ppm. ¹³C NMR (CDCl₃, 101 MHz): 136.9, 136.6, 136.3, 134.7, 132.3, 131.9, 131.6, 131.2, 130.4, 128.8, 128.4, 124.5, 123.9, 122.3, 90.3, 89.5, 81.1, 74.6 ppm. HRESI-MS (pos.): 1433.3948, calculated for [C₁₀₈H₅₈Si₂Na]⁺, i.e. [1-Na]⁺ = 1433.3975 Da.

Synthesis of 1-Co₂₄(CO)₇₂: A Schlenk flask charged with **1** (0.010 g, 0.0070 mmol) was transferred to a glove box and Co₂(CO)₈ (0.048 g, 0.14 mmol) was added. The reaction flask was sealed and dry THF (3 mL) was added outside the glove box. The reaction mixture was stirred in the dark for 5 h under a nitrogen atmosphere. The reaction was quenched with cold EtOH (1 mL) and the solvent was evaporated under a stream nitrogen. The resulting black residue was dissolved in DCM (5 mL) and filtered through a cotton plug. The solvent was removed under reduced pressure to give **1-Co₂₄(CO)₇₂** as a dark brown powder. Yield: 0.023 g (0.0047 mmol, 67%). ¹H NMR (CD₂Cl₂, 400 MHz): 7.74 (s, 6H), 7.38–7.70 (m, 46H), 7.28 (t, *J* = 7.8 Hz, 6H) ppm. ¹³C NMR (CD₂Cl₂, 151 MHz): 199.5, 199.0, 140.4, 140.1, 139.9, 137.2, 136.8, 134.2, 133.7, 131.5, 130.4, 129.1, 129.0, 128.7, 128.5, 128.4, 99.7, 93.6, 91.9, 91.5 ppm. IR (CH₂Cl₂, *inter alia*): 2091, 2052, 2022 cm⁻¹ (C≡O stretch). HRESI-MS (pos.): 4863.4312, calc. for [C₁₈₀H₅₈O₇₂Si₂Co₂₄Na]⁺, i.e. [1-Co₂₄(CO)₇₂Na]⁺ = 4863.4281 Da.

Acknowledgements

We thank the Australian National University (PhD scholarship to CMT) and Australian Research Council (FT210100495 to NGW) for funding, Prof. Anthony Hill and Prof. Michelle Coote for useful discussions, and Anitha Jeyasingham for assistance with mass spectrometry. Parts of this work were conducted on the MX2 beamline of the Australian Synchrotron^[26] and made use of the Australian Cancer Research Foundation detector. Parts of this research were undertaken using the National Computational Infrastructure (NCI), which is supported by the Australian Government. Open Access publishing facilitated by Australian National University, as part of the Wiley - Australian National University agreement via the Council of Australian University Librarians.

Conflict of Interest

The authors declare no conflict of interest.

Data Availability Statement

The data that support the findings of this study are available in the supplementary material of this article.

Keywords: alkynes · cages · cobalt · porosity · post-synthetic modification

- [1] a) M. Yoshizawa, J. K. Klosterman, M. Fujita, *Angew. Chem. Int. Ed.* **2009**, *48*, 3418–3438; *Angew. Chem.* **2009**, *121*, 3470–3490; b) M. M. J. Smulders, I. A. Riddell, C. Browne, J. R. Nitschke, *Chem. Soc. Rev.* **2013**, *42*, 1728–1754; c) T. R. Cook, P. J. Stang, *Chem. Rev.* **2015**, *115*, 7001–7045.
- [2] a) X. Liu, Y. Liu, G. Li, R. Warmuth, *Angew. Chem. Int. Ed.* **2006**, *45*, 901–904; *Angew. Chem.* **2006**, *118*, 915–918; b) O. Francesconi, A. Ienco, G. Moneti, C. Nativi, S. Roelens, *Angew. Chem. Int. Ed.* **2006**, *45*, 6693–6696; *Angew. Chem.* **2006**, *118*, 6845–6848; c) P. Skowronek, J. Gawronski, *Org. Lett.* **2008**, *10*, 4755–4758; d) N. Nishimura, K. Kobayashi, *Angew. Chem. Int. Ed.* **2008**, *47*, 6255–6258; *Angew. Chem.* **2008**, *120*, 6351–6354; e) N. Christinat, R. Scopelliti, K. Severin, *Angew. Chem. Int. Ed.* **2008**, *47*, 1848–1852; *Angew. Chem.* **2008**, *120*, 1874–1878; f) T. Tozawa, J. T. A. Jones, S. I. Swamy, S. Jiang, D. J. Adams, S. Shakespeare, R. Clowes, D. Bradshaw, T. Hasell, S. Y. Chong, C. Tang, S. Thompson, J. Parker, A. Trewin, J. Bacsa, A. M. Z. Slawin, A. Steiner, A. I. Cooper, *Nat. Mater.* **2009**, *8*, 973; g) M. Mastalerz, *Angew. Chem. Int. Ed.* **2010**, *49*, 5042–5053; *Angew. Chem.* **2010**, *122*, 5164–5175; h) G. Zhang, M. Mastalerz, *Chem. Soc. Rev.* **2014**, *43*, 1934–1947; i) G. Zhang, O. Presly, F. White, I. M. Oppel, M. Mastalerz, *Angew. Chem. Int. Ed.* **2014**, *53*, 1516–1520; *Angew. Chem.* **2014**, *126*, 1542–1546; j) T. Hasell, A. I. Cooper, *Nat. Rev. Mater.* **2016**, *1*, 16053; k) S. Bera, K. Dey, T. K. Pal, A. Halder, S. Tothadi, S. Karak, M. Addicoat, R. Banerjee, *Angew. Chem. Int. Ed.* **2019**, *58*, 4243–4247; *Angew. Chem.* **2019**, *131*, 4287–4291.
- [3] a) C. Zhang, C.-F. Chen, *J. Org. Chem.* **2007**, *72*, 9339–9341; b) A. Avellaneda, P. Valente, A. Burgun, J. D. Evans, A. W. Markwell-Heys, D. Rankine, D. J. Nielsen, M. R. Hill, C. J. Sumbly, C. J. Doonan, *Angew. Chem. Int. Ed.* **2013**, *52*, 3746–3749; *Angew. Chem.* **2013**, *125*, 3834–3837; c) M. Tominaga, K. Ohara, K. Yamaguchi, I. Azumaya, *J. Org. Chem.* **2014**, *79*, 6738–6742; d) H. Ma, T.-L. Zhai, Z. Wang, G. Cheng, B. Tan, C. Zhang, *RSC Adv.* **2020**, *10*, 9088–9092; e) Z.-Q. Zhang, Q.-X. Ren, W.-F. Tian, W.-H. Sun, X.-P. Cao, Z.-F. Shi, H.-F. Chow, D. Kuck, *Org. Lett.* **2021**, *23*, 1478–1483.
- [4] We note that Moore has pioneered the synthesis of cages using alkyne metathesis, which in some ways may be said to combine the best of both worlds in that it combines a reversible (and thus thermodynamically-controlled) reaction but gives a product containing a chemically robust alkyne group. See: a) S. Lee, A. Yang, T. P. Money Penny II, J. S. Moore, *J. Am. Chem. Soc.* **2016**, *138*, 2182–2185; b) C. Pattillo, J. S. Moore, *Chem. Sci.* **2019**, *10*, 7043–7048. Hydrazone chemistry may offer similar opportunities: c) M. Yang, F. Qiu, E.-S. M. El-Sayed, W. Wang, S. Du, K. Su, D. Yuan, *Chem. Sci.* **2021**, *12*, 13307–13315.
- [5] a) J. T. A. Jones, T. Hasell, X. Wu, J. Bacsa, K. E. Jelfs, M. Schmidtman, S. Y. Chong, D. J. Adams, A. Trewin, F. Schiffman, F. Cora, B. Slater, A. Steiner, G. M. Day, A. I. Cooper, *Nature* **2011**, *474*, 367–371; b) T. Anglim Lagones, S. A. Boer, N. G. White, *Cryst. Growth Des.* **2019**, *19*, 4121–4126; c) G. A. Taggart, A. M. Antonio, G. R. Lorzing, G. P. A. Yap, E. D. Bloch, *ACS Appl. Mater. Interfaces* **2020**, *12*, 24913–24919; d) A. J. Gosselin, G. E. Decker, A. M. Antonio, G. R. Lorzing, G. P. A. Yap, E. D. Bloch, *J. Am. Chem. Soc.* **2020**, *142*, 9594–9598.
- [6] M. Kitchin, K. Konstantas, C. J. Sumbly, M. L. Czyn, P. Valente, M. R. Hill, A. Polyzos, C. J. Doonan, *Chem. Commun.* **2015**, *51*, 14231–14234.
- [7] a) Z. Wang, S. M. Cohen, *Chem. Soc. Rev.* **2009**, *38*, 1315–1329; b) S. Mandal, S. Natarajan, P. Mani, A. Pankajakshan, *Adv. Funct. Mater.* **2021**, *31*, 2006291.
- [8] H. Wang, Y. Jin, N. Sun, W. Zhang, J. Jiang, *Chem. Soc. Rev.* **2021**, *50*, 8874–8886.
- [9] a) T. Hasell, X. Wu, J. T. A. Jones, J. Bacsa, A. Steiner, T. Mitra, A. Trewin, D. J. Adams, A. I. Cooper, *Nat. Chem.* **2010**, *2*, 750–755; b) J. L. Culshaw, G. Cheng, M. Schmidtman, T. Hasell, M. Liu, D. J. Adams, A. I. Cooper, *J. Am. Chem. Soc.* **2013**, *135*, 10007–10010; c) Q.-Q. Wang, N. Luo, X.-D. Wang, Y.-F. Ao, Y.-F. Chen, J.-M. Liu, C.-Y. Su, D.-X. Wang, M.-X. Wang, *J. Am. Chem. Soc.* **2017**, *139*, 635–638; d) A. S. Bhat, S. M. Elbert, W.-S. Zhang, F. Rominger, M. Dieckmann, R. R. Schröder, M. Mastalerz, *Angew. Chem. Int. Ed.* **2019**, *58*, 8819–8823; *Angew. Chem.* **2019**, *131*, 8911–8915.
- [10] a) R. McCaffrey, H. Long, Y. Jin, A. Sanders, W. Park, W. Zhang, *J. Am. Chem. Soc.* **2014**, *136*, 1782–1785; b) J.-K. Sun, W.-W. Zhan, T. Akita, Q. Xu, *J. Am. Chem. Soc.* **2015**, *137*, 7063–7066; c) B. Mondal, K. Acharyya, P. Howlader, P. S. Mukherjee, *J. Am. Chem. Soc.* **2016**, *138*, 1709–1716; d) L. Qiu, R. McCaffrey, Y. Jin, Y. Gong, Y. Hu, H. Sun, W. Park, W. Zhang, *Chem. Sci.* **2018**, *9*, 676–680; e) M. Nihei, H. Ida, T. Nibe, A. M. P. Moeljadi, Q. T. Trinh, H. Hira, M. Ishizaki, M. Kurihara, T. Shiga, H. Oshio, *J. Am. Chem. Soc.* **2018**, *140*, 17753–17759.
- [11] a) S. I. Swamy, J. Bacsa, J. T. A. Jones, K. C. Stylianou, A. Steiner, L. K. Ritchie, T. Hasell, J. A. Gould, A. Laybourn, Y. Z. Khimiyak, D. J. Adams, M. J. Rosseinsky, A. I. Cooper, *J. Am. Chem. Soc.* **2010**, *132*, 12773–12775; b) L. Zhang, L. Xiang, C. Hang, W. Liu, W. Huang, Y. Pan, *Angew. Chem. Int. Ed.* **2017**, *56*, 7787–7791; *Angew. Chem.* **2017**, *129*, 7895–7899; c) Y. Kim, J. Koo, I.-C. Hwang, R. D. Mukhopadhyay, S. Hong, J. Yoo, A. A. Dar, I. Kim, D. Moon, T. J. Shin, Y. H. Ko, K. Kim, *J. Am. Chem. Soc.* **2018**, *140*, 14547–14551.
- [12] a) S. Akine, M. Miyashita, T. Nabeshima, *J. Am. Chem. Soc.* **2017**, *139*, 4631–4634; b) P. T. Smith, B. P. Benke, Z. Cao, Y. Kim, E. M. Nichols, K. Kim, C. J. Chang, *Angew. Chem. Int. Ed.* **2018**, *57*, 9684–9688; *Angew. Chem.* **2018**, *130*, 9832–9836; c) M. M. Deegan, R. Bhattacharjee, S. Caratzoulas, E. D. Bloch, *Inorg. Chem.* **2021**, *60*, 7044–7050.
- [13] H. Greenfield, H. W. Sternberg, R. A. Friedel, J. H. Wotiz, R. Markby, I. Wender, *J. Am. Chem. Soc.* **1956**, *78*, 120–124.
- [14] A. L. Spek, *Acta Crystallogr. Sect. C* **2015**, *71*, 9–18.
- [15] S. A. Boer, L.-J. Yu, T. L. Genet, K. Low, D. A. Cullen, M. G. Gardiner, M. L. Coote, N. G. White, *Chem. Eur. J.* **2021**, *27*, 1768–1776.
- [16] A. Burgun, P. Valente, J. D. Evans, D. M. Huang, C. J. Sumbly, C. J. Doonan, *Chem. Commun.* **2016**, *52*, 8850–8853.
- [17] A similar phenomenon has also been reported for a triptycene-based hydrocarbon cage, see Ref. [3d].
- [18] D. Eisler, W. Hong, M. C. Jennings, R. J. Puddephatt, *Organometallics* **2002**, *21*, 3955–3960.
- [19] S. Aime, L. Milone, R. Rossetti, P. L. Stanghellini, *Inorg. Chim. Acta* **1977**, *22*, 135–139.
- [20] R. L. Sweeney, T. L. Brown, *Inorg. Chem.* **1977**, *16*, 415–421.
- [21] a) P. H. Bird, A. R. Fraser, D. N. Hall, *Inorg. Chem.* **1977**, *16*, 1923–1931; b) D. R. Kohn, P. Gawel, Y. Xiong, K. E. Christensen, H. L. Anderson, *J. Org. Chem.* **2018**, *83*, 2077–2086.
- [22] C. Bannwarth, S. Ehlert, S. Grimme, *J. Chem. Theory Comput.* **2019**, *15*, 1652–1671.
- [23] C. Bannwarth, E. Caldeweyher, S. Ehlert, A. Hansen, P. Pracht, J. Seibert, S. Spicher, S. Grimme, *WIREs Comput. Mol. Sci.* **2021**, *11*, e1493.
- [24] R. Taylor, P. A. Wood, *Chem. Rev.* **2019**, *119*, 9427–9477.
- [25] a) A. Rit, T. Pape, F. E. Hahn, *J. Am. Chem. Soc.* **2010**, *132*, 4572–4573; b) Y.-S. Wang, T. Feng, Y.-Y. Wang, F. E. Hahn, Y.-F. Han, *Angew. Chem. Int. Ed.* **2018**, *57*, 15767–15771; *Angew. Chem.* **2018**, *130*, 15993–15997; c) M.-M. Gan, J.-Q. Liu, L. Zhang, Y.-Y. Wang, F. E. Hahn, Y.-F. Han, *Chem. Rev.* **2018**, *118*, 9587–9641; d) S. Ibáñez, E. Peris, *Angew. Chem. Int. Ed.* **2019**, *58*, 6693–6697; *Angew. Chem.* **2019**, *131*, 6765–6769.
- [26] D. Aragao, J. Aishima, H. Cherukuvada, R. Clarken, M. Clift, N. P. Cowieson, D. J. Ericsson, C. L. Gee, S. Macedo, N. Mudie, S. Panjikar, J. R. Price, A. Riboldi-Tunncliffe, R. Rostan, R. Williamson, T. T. Caradoc-Davies, *J. Synchrotron Radiat.* **2018**, *25*, 885–891.

Manuscript received: March 28, 2022
Version of record online: July 21, 2022